

DUAL WEIGHTED RESIDUAL ERROR CONTROL FOR FRICTIONAL CONTACT PROBLEMS.

ANDREAS RADEMACHER* AND ANDREAS SCHRÖDER†

Abstract. In this paper goal-oriented error control based on dual weighted residual error estimations (DWR) is applied to frictional contact problems. A mixed formulation of the contact problem is used to derive a discretization. It relies on the introduction of Lagrange multipliers to capture the frictional contact conditions. The discretization error is estimated in terms of functionals (the quantities of interest) which are evaluated in the displacement field as well as the Lagrange multipliers. Numerical experiments confirm the applicability of the estimates within adaptive schemes.

Key words. error estimation, dual weighted residual, contact, friction, mixed formulation

AMS subject classifications. 65N30, 65N15

1. Introduction. Modern finite element schemes commonly include a posteriori error control and adaptivity. One of the most popular techniques from the last decades to derive error estimates for user-defined, probably non-linear error measures (quantities of interest) is known as the dual weighted residual method (DWR), c.f. [1, 2]. It relies on representing the error in terms of the solution of a dual problem. Such duality arguments are the basis of many techniques in so-called goal-oriented error control. We refer to [13, 14] for further approaches similar to the DWR method.

In this paper, the DWR method is applied to frictional contact problems, which play an important role in mechanical engineering, cf. [7, 12]. Variational formulations of contact problems are given by variational inequalities or by variational equations in combination with penalty or regularization approaches, cf. [12]. The DWR method is already successfully applied to these two formulations of contact problems, cf. [19]. A third variant to variationally formulate frictional contact problems is given by mixed methods where the geometrical and frictional contact conditions are captured by Lagrange multipliers. This approach has mainly two advantages: First, the Lagrange multipliers can be interpreted as normal and tangential contact forces which enables to directly determine these quantities. Second, the constraints of the Lagrange multipliers are sign conditions and box constraints which appear simpler than the contact conditions of primal formulations and enables solution schemes without penalty or regularization parameters. The application of the DWR method to contact problems in such a mixed setting has been rarely studied so far, see, e.g., [18, 19]. In particular, the control of the error in terms of the Lagrange multipliers has not been discussed in literature up to now. Our aim is, therefore, to derive DWR estimates for mixed formulations of frictional contact problems and, in particular, for error functionals which measure the error of the displacement field *as well as* the Lagrange multipliers. Due to the interpretation of the Lagrange multipliers as contact forces this error control is of special interest in many applications.

In this paper, we use a mixed discretization scheme proposed by Haslinger et al. for frictional contact problems with Tresca friction, cf. [11]. In this low-order approach the displacement field is discretized by the usual low-order conforming ansatz and the Lagrange multiplier by piecewise constant functions. The unique existence of the

*Institute of Applied Mathematics, Technische Universität Dortmund, 44221 Dortmund, Germany, (andreas.rademacher@tu-dortmund.de).

†Department of Mathematics, Humboldt-Universität zu Berlin, 10099 Berlin, Germany, (schroder@math.hu-berlin.de).

discrete solution is verified via an inf-sup condition associated to the discretization spaces for the displacement and the Lagrange multipliers which possibly requires the use of a boundary mesh with a larger mesh size than that of the interior mesh, cf. [9]. The proposed discretization scheme is widely studied and enhanced by Haslinger et al. [8, 10] for many applications in frictional contact problems.

In a first step, we estimate the error in terms of a functional which only depends on the displacement field. The dual problem is then given as the Riesz representation in terms of the bilinear form introduced within the mixed variational formulation of the problem. We obtain an error representation consisting of primal and dual residuals as well as a remainder coming from the trapezoidal rule as in the standard DWR approach for variational equations. In addition, the representation contains a term which measures the error in the contact conditions. In a second step, we estimate the error in both variables, the displacement field and the Lagrange multipliers. For this purpose, we extend the dual problem to a mixed problem. Again, we obtain the usual residuals of the DWR method and a term for the error in the contact conditions.

As usual in the DWR method, the residuals are approximated. We use quadratic interpolations on coarser, patch-structured meshes, cf. [1]. The additional contact terms are approximated by some interpolation and averaging techniques.

The paper is organized as follows: After the introduction of some notational conventions in Section 2, we give a short overview of contact problems with Tresca friction and of their mixed variational formulation in Section 3. Section 4 focuses on the low-order discretization scheme as proposed by Haslinger et al. In Section 5, we discuss the DWR error control for the displacement field whereas Section 6 introduces the error control of both variables, the displacement field and the Lagrange multipliers. Approximation and localization techniques for the derived error representations are discussed in Section 7. Finally, the numerical experiments of Section 8 confirm the applicability of the theoretical findings. In particular, we demonstrate the approach for numerical examples where the Lagrange multipliers directly defines the quantity of interest.

2. Notations. Let $\Omega \subset \mathbb{R}^k$, $k = 2, 3$, be a domain with sufficiently smooth boundary $\Gamma := \partial\Omega$. Moreover, let $\Gamma_D \subset \Gamma$ be closed with positive measure and let $\Gamma_C \subset \Gamma \setminus \Gamma_D$ with $\bar{\Gamma}_C \subsetneq \bar{\Gamma} \setminus \Gamma_D$. $L^2(\Omega)$, $H^l(\Omega)$ with $l \geq 1$, and $H^{1/2}(\Gamma_C)$ denote the usual Sobolev spaces and we set $H_D^1(\Omega) := \{v \in H^1(\Omega) \mid \gamma(v) = 0 \text{ on } \Gamma_D\}$ and $V := H_D^1(\Omega; \mathbb{R}^k)$ with the trace operator γ . The space $\tilde{H}^{-1/2}(\Gamma_C)$ denotes the topological dual space of $H^{1/2}(\Gamma_C)$ with the norms $\|\cdot\|_{-1/2, \Gamma_C}$ and $\|\cdot\|_{1/2, \Gamma_C}$, respectively. Let $(\cdot, \cdot)_{0, \omega}$, $(\cdot, \cdot)_{0, \Gamma'}$ be the usual L^2 -scalar products on $\omega \subset \Omega$ and $\Gamma' \subset \Gamma$. Note that the linear and bounded mapping $\gamma_C := \gamma|_{\Gamma_C} : H_D^1(\Omega) \rightarrow H^{1/2}(\Gamma_C)$ is surjective due to the assumptions on Γ_C , cf. [12, p.88]. For functions in $L^2(\Gamma_C)$, the inequality symbols \geq and \leq are defined as ‘‘almost everywhere’’. We set $H_+^{1/2}(\Gamma_C) := \{v \in H^{1/2}(\Gamma_C) \mid v \geq 0\}$. Furthermore, we define the dual cone of $H_+^{1/2}(\Gamma_C)$ by $\Lambda_n := \{\mu \in \tilde{H}^{-1/2}(\Gamma_C) \mid \forall v \in H_+^{1/2}(\Gamma_C) : \langle \mu, v \rangle \geq 0\}$ and $\Lambda_t := \{\mu \in L^2(\Gamma_C; \mathbb{R}^{k-1}) \mid |\mu| \leq 1 \text{ on } \text{supp } s, v = 0 \text{ on } \Gamma_C \setminus \text{supp } s\}$ with the euclidian norm $|\cdot|$ and $s \in L^2(\Gamma_C)$, $s \geq 0$. For the displacement field $v \in V$, we specify the linearized strain tensor as $\varepsilon(v) := \frac{1}{2}(\nabla v + (\nabla v)^\top)$ and the stress tensor as $\sigma(v)_{ij} := \mathcal{C}_{ijkl}\varepsilon(v)_{kl}$ describing a linear-elastic material law where $\mathcal{C}_{ijkl} \in L^\infty(\Omega)$ with $\mathcal{C}_{ijkl} = \mathcal{C}_{jikl} = \mathcal{C}_{klij}$ and $\mathcal{C}_{ijkl}\tau_{ij}\tau_{kl} \geq \kappa\tau_{ij}^2$ for $\tau \in L^2(\Omega)_{\text{sym}}^{k \times k}$ and a $\kappa > 0$. In the following n denotes the vector-valued function describing the outer unit normal vector with respect to Γ and t the $k \times (k-1)$ -matrix-valued function containing the tangential vectors. We define

$\sigma_{n,j} := \sigma_{ij}n_i$, $\sigma_{nn} := \sigma_{ij}n_in_j$, $\sigma_{nt,l} := \sigma_{ij}n_it_{jl}$, $v_n := \gamma_C(v_i)n_i$ and $v_{t,j} := \gamma_C(v_i)t_{ij}$. Furthermore, we set $v_N := \gamma_{|\Gamma_N}(v)$ and $v_C := \gamma_C(v)$ for $v \in V$.

3. The mixed formulation of Signorini's problem with Tresca friction.

Signorini's problem with Tresca friction is to find a displacement field $u \in V$ such that

$$-\operatorname{div}(\sigma(u)) = f \text{ in } \Omega, \quad \sigma_n(u) = b \text{ on } \Gamma_N, \quad (3.1)$$

$$u_n - g \leq 0, \quad \sigma_{nn}(u) \leq 0, \quad \sigma_{nn}(u)(u_n - g) = 0 \text{ on } \Gamma_C, \quad (3.2)$$

$$|\sigma_{nt}(u)| \leq s \text{ with } \left\{ \begin{array}{l} |\sigma_{nt}(u)| < s \Rightarrow u_t = 0, \\ |\sigma_{nt}(u)| = s \Rightarrow \exists \zeta \in \mathbb{R}_{\geq 0} : u_t = -\zeta \sigma_{nt}(u) \end{array} \right\} \text{ on } \Gamma_C \quad (3.3)$$

where we assume that $f \in L^2(\Omega)$, $b \in L^2(\Gamma_N)$, $g \in H^{1/2}(\Gamma_C)$ and $s \in L^2(\Gamma_C)$ with $s \geq 0$. Equation (3.1) is the usual equilibrium equation of linear elasticity with the volume and surface loads f and b . The conditions in (3.2) describes the geometrical contact: We assume that Γ_C is parameterized by a sufficiently smooth function $\varphi : \mathbb{R}^{k-1} \rightarrow \mathbb{R}$ such that, without loss of generality, the geometrical contact condition for a displacement field v in the k -th component is given by $\varphi(x) + v_k(x, \varphi(x)) \leq \psi(x_1 + v_1(x, \varphi(x)), \dots, x_{k-1} + v_{k-1}(x, \varphi(x)))$ with $x := (x_1, \dots, x_{k-1}) \in \mathbb{R}^{k-1}$ and a sufficiently smooth function ψ describing the surface of an obstacle. The linearization of this condition gives us $v_n \leq g$ in (3.2) with $g(x) := (\psi(x) - \varphi(x))(1 + (\nabla\varphi(x))^\top \nabla\varphi(x))^{-1/2}$, cf. [12, Ch. 2]. The second condition is a sign condition for the normal contact force describing pressure. The complementary condition in (3.2) describes either pressure or no contact. The condition of Tresca friction can be found in (3.3). It turns out that sliding does not occur if the magnitude of the tangential forces is below a critical value given by the frictional function s . If the tangential forces reach this critical value, sliding is obtained in the negative direction of the tangential forces. Setting s to the magnitude of the normal forces times a friction coefficient, Tresca friction is extended to Coulomb friction, see Section 8.

With the symmetric, continuous and V -elliptic bilinearform $a(w, v) := (\sigma(w), \varepsilon(v))_0$ on $V \times V$ as well as the continuous linearform $\langle \ell, v \rangle := (f, v)_0 + (b, v_N)_{0, \Gamma_N}$ and using some standard arguments of convex analysis (c.f., e.g., [5, 6, 12, 17]), we obtain that the triple $(u, \lambda_n, \lambda_t) \in V \times \Lambda_n \times \Lambda_t$ is a saddle point of the frictional contact problem (3.1)-(3.3) if and only if,

$$\begin{aligned} a(u, v) &= \langle \ell, v \rangle - \langle \lambda_n, v_n - g \rangle - (\lambda_t, sv_t)_{0, \Gamma_C}, \\ \langle \mu_n - \lambda_n, u_n - g \rangle + (\mu_t - \lambda_t, su_t)_{0, \Gamma_C} &\leq 0 \end{aligned} \quad (3.4)$$

for all $v \in V$ and all $(\mu_n, \mu_t) \in \Lambda_n \times \Lambda_t$. Note that a unique solution exists under the assumptions as introduced in this Section and Section 2. Moreover, the Lagrange multiplier λ_n coincides with the normal contact stress $-\sigma_{nn}(u)$ as well as λ_t with the tangential contact stress $-\sigma_{nt}(u)$.

4. Low-order discretization. Let \mathcal{T} be a finite element mesh of Ω with mesh size h and let \mathcal{E}_C be a finite element mesh of Γ_C with mesh size H , respectively. The number of mesh elements in \mathcal{T} is denoted by M_Ω and in \mathcal{E}_C by M_C . We use line segments, quadrangles or hexahedrons to define \mathcal{T} or \mathcal{E}_C . But this is not a restriction, triangles and tetrahedrons are also possible. We assume that a submesh of \mathcal{E}_C is a mesh of $\operatorname{supp} s$. Furthermore, let $\Psi_T : [-1, 1]^k \rightarrow T \in \mathcal{T}$ and $\Phi_E : [-1, 1]^{k-1} \rightarrow E \in$

\mathcal{E}_C be affine and k -linear transformations. We define

$$\begin{aligned} V_h &:= \{v \in V \mid \forall T \in \mathcal{T} : v|_T \circ \Psi_T \in Q_1\}, \\ M_H &:= \{\mu \in L^2(\Gamma_C) \mid \forall E \in \mathcal{E}_C : \mu|_E \circ \Phi_E \in P_0\}, \end{aligned}$$

where Q_1 is the set of k -linear functions on $[-1, 1]^k$ and P_0 the set of constant functions on $[-1, 1]^{k-1}$. Moreover, we define

$$\begin{aligned} \Lambda_{n,H} &:= \{\mu \in M_H \mid \forall E \in \mathcal{E}_C : \mu \geq 0\}, \\ \Lambda_{t,H} &:= \{\mu \in (M_H)^{k-1} \mid \forall E \in \mathcal{E}_C, E \subset \text{supp } s : |\mu| \leq 1, \\ &\quad \mu = 0 \text{ on } \Gamma_C \setminus \text{supp } s\}. \end{aligned}$$

The discrete saddle point problem is to find $(u_h, \lambda_{n,H}, \lambda_{t,H}) \in V_h \times \Lambda_{n,H} \times \Lambda_{t,H}$ such that

$$\begin{aligned} a(u_h, v_h) &= \langle \ell, v_h \rangle - \langle \lambda_{n,H}, v_{h,n} \rangle - (\lambda_{t,H}, sv_{h,t})_{0,\Gamma_C}, \\ \langle \mu_{n,H} - \lambda_{n,H}, u_{h,n} - g \rangle &+ (\mu_{t,H} - \lambda_{t,H}, su_{h,t})_{0,\Gamma_C} \leq 0 \end{aligned} \quad (4.1)$$

for all $v_h \in V_h$ and all $(\mu_{n,H}, \mu_{t,H}) \in \Lambda_{n,H} \times \Lambda_{t,H}$. It is well-known, that there exists a unique discrete saddle point $(u_h, \lambda_{n,H}, \lambda_{t,H}) \in V_h \times \Lambda_{n,H} \times \Lambda_{t,H}$, if a discrete inf-sup condition is fulfilled. In the case of quasi-uniform meshes the discrete inf-sup condition holds if the quotient of the mesh sizes h/H is sufficiently small, cf. [9]. It is noted that different mesh sizes h and H implies that the Lagrange multiplier is defined on a coarser mesh which may lead to a higher implementational complexity than using a surface mesh \mathcal{E}_C which is inherited from the interior mesh \mathcal{T} . In compliance with the mentioned reference, we observe in our experiments that the choice $H = h$ leads to oscillating Lagrange multipliers whereas $H = 2h$ results in a stable scheme. Thus, we use meshes with $H = 2h$ in the experiments of Section 8.

Note, in the mixed method as proposed in this section, the Galerkin orthogonality with respect to u and u_h is not valid. Instead, we have the following statement.

LEMMA 4.1. *The identity*

$$a(u - u_h, v_h) = \langle \lambda_{n,H} - \lambda_n, v_{h,n} \rangle + (\lambda_{t,H} - \lambda_t, sv_{h,t})_{0,\Gamma_C}$$

holds for an arbitrary $v_h \in V_h$.

Proof. There holds $a(u, v_h) = \langle \ell, v_h \rangle - \langle \lambda_n, v_{h,n} \rangle - (\lambda_t, sv_{h,t})_{0,\Gamma_C}$ and $a(u_h, v_h) = \langle \ell, v_h \rangle - \langle \lambda_{n,H}, v_{h,n} \rangle - (\lambda_{t,H}, sv_{h,t})_{0,\Gamma_C}$. Subtracting yields the assertion. \square

5. Error estimation of the displacement field. In this section, we consider a user-defined functional $J_u : V \rightarrow \mathbb{R}$, which measures some quantity of physical interest only in the displacement field. The essentially more complicated case where the functional depends on the displacement field *and* the Lagrange multipliers is considered in the next section. In the following, we assume that J_u is (three times) Fréchet-differentiable and $J'_u : V \rightarrow V^*$ denotes its derivative.

The aim of goal-oriented error control is to approximatively determine or to estimate $J_u(u) - J_u(u_h)$. In the concept of dual weighted residual error estimations, this is done through the representation of J_u by the solution of a dual problem which is given by the following variational formulation: We seek $z \in V$, such that

$$a(v, z) = \langle J'_u(u), v \rangle \quad (5.1)$$

for all $v \in V$. An approximation is given by $z_h \in V_h$ fulfilling

$$a(v_h, z_h) = \langle J'_u(u_h), v_h \rangle \quad (5.2)$$

for all $v_h \in V_h$. Note that the unique existence of solutions z and z_h of (5.1) and (5.2) is guaranteed by standard arguments.

The basic idea of the DWR method is to determine the error in terms of the primal and dual residuals $\text{Res} : V \rightarrow V^*$ and $\text{Res}_u^* : V \rightarrow V^*$. Here, we define them as

$$\begin{aligned} \langle \text{Res}(w), v \rangle &:= \ell(v) - (\lambda_{n,H}, v_n)_{0,\Gamma_C} - (\lambda_{t,H}, v_t)_{0,\Gamma_C} - a(w, v), \\ \langle \text{Res}_u^*(w), v \rangle &:= \langle J'_u(u_h), v \rangle - a(v, w). \end{aligned}$$

Obviously, there holds

$$\langle \text{Res}(u_h), v_h \rangle = \langle \text{Res}_u^*(z_h), v_h \rangle = 0 \quad (5.3)$$

for all $v_h \in V_h$. From the fundamental theorem of calculus and the trapezoidal rule, we deduce

$$\begin{aligned} J_u(u) - J_u(u_h) &= \int_0^1 \langle J'(u + \kappa(u - u_h)), u - u_h \rangle d\kappa \\ &= \frac{1}{2} (\langle J'(u), u - u_h \rangle + \langle J'_u(u_h), u - u_h \rangle) + R_u(u - u_h) \end{aligned} \quad (5.4)$$

with the remainder

$$R_u(v) := \frac{1}{2} \int_0^1 \langle (J_u'''(u_h + \kappa v))(v)(v), v \rangle \kappa(\kappa - 1) d\kappa$$

and the third derivative $J_u''' : V \rightarrow \mathcal{L}(V, \mathcal{L}(V, V^*))$ of J .

LEMMA 5.1. *The equation*

$$a(u - u_h, z) = \langle \text{Res}(u_h), z - \tilde{z}_h \rangle - \langle \lambda_n - \lambda_{n,H}, z_n \rangle - (\lambda_t - \lambda_{t,H}, sz_t)_{0,\Gamma_C}$$

is satisfied for an arbitrary $\tilde{z}_h \in V_h$.

Proof. From (5.3) we obtain

$$\begin{aligned} a(u - u_h, z) &= \langle \ell, z \rangle - \langle \lambda_n, z_n \rangle - (\lambda_t, sz_t)_{0,\Gamma_C} - a(u_h, z) \\ &= \langle \ell, z \rangle - \langle \lambda_{n,H}, z_n \rangle - (\lambda_{t,H}, sz_t)_{0,\Gamma_C} - a(u_h, z) \\ &\quad + \langle \lambda_{n,H} - \lambda_n, z_n \rangle + (\lambda_{t,H} - \lambda_t, sz_t)_{0,\Gamma_C} \\ &= \langle \text{Res}(u_h), z - \tilde{z}_h \rangle - \langle \lambda_n - \lambda_{n,H}, z_n \rangle - (\lambda_t - \lambda_{t,H}, sz_t)_{0,\Gamma_C}. \end{aligned}$$

□

Using Lemma 5.1, we obtain the following error representation.

THEOREM 5.2. *There holds*

$$J_u(u) - J_u(u_h) = \frac{1}{2} \langle \text{Res}(u_h), z - \tilde{z}_h \rangle + \frac{1}{2} \langle \text{Res}_u^*(z_h), u - \tilde{u}_h \rangle + \rho^* + R_u(u - u_h)$$

for arbitrary $\tilde{z}_h, \tilde{u}_h \in V_h$ where

$$\rho^* := \langle \lambda_{n,H} - \lambda_n, \frac{1}{2}(z_n + z_{h,n}) \rangle + (\lambda_{t,H} - \lambda_t, s \frac{1}{2}(z_t + z_{h,t}))_{0,\Gamma_C}.$$

Proof. For $e := u - u_h$, $e_n^\lambda := \lambda_n - \lambda_{n,H}$ and $e_t^\lambda := \lambda_t - \lambda_{t,H}$, we obtain from Lemma 5.1 and (5.3)

$$\begin{aligned} & a(e, z) + \langle J'_u(u_h), e \rangle \\ &= \langle \text{Res}(u_h), z - \tilde{z}_h \rangle + \langle J'_u(u_h), e \rangle - \langle e_n^\lambda, z_n \rangle - (e_t^\lambda, z_t)_{0, \Gamma_C} \\ &= \langle \text{Res}(u_h), z - \tilde{z}_h \rangle + \langle J'_u(u_h), e \rangle - a(e, z_h) \\ &\quad - \langle e_n^\lambda, z_{h,n} \rangle - (e_t^\lambda, z_{h,t})_{0, \Gamma_C} - \langle e_n^\lambda, z_n \rangle - (e_t^\lambda, z_t)_{0, \Gamma_C} \\ &= \langle \text{Res}(u_h), z - \tilde{z}_h \rangle + \langle \text{Res}_u^*(z_h), u - \tilde{u}_h \rangle + 2\rho^*. \end{aligned}$$

Using (5.4), we finally obtain

$$\begin{aligned} J_u(u) - J_u(u_h) &= \frac{1}{2} (\langle J'_u(u), e \rangle + \langle J'_u(u_h), e \rangle) + R_u(u - u_h) \\ &= \frac{1}{2} (a(e, z) + \langle J'_u(u_h), e \rangle) + R_u(u - u_h) \\ &= \frac{1}{2} \langle \text{Res}(u_h), z - \tilde{z}_h \rangle + \frac{1}{2} \langle \text{Res}_u^*(z_h), u - u_h \rangle + \rho^* + R_u(u - u_h). \end{aligned}$$

□

If J is linear, the remainder $R_u(u - u_h)$ vanishes and the error representation in Theorem 5.2 simplifies to the following statement.

COROLLARY 5.3. *If $J_u \in V^*$ then the identities*

$$\begin{aligned} J_u(u) - J_u(u_h) &= \frac{1}{2} \langle \text{Res}(u_h), z - \tilde{z}_h \rangle + \frac{1}{2} \langle \text{Res}_u^*(z_h), u - \tilde{u}_h \rangle + \rho^* \\ &= \langle \text{Res}(u_h), z - \tilde{z}_h \rangle + \hat{\rho}^* \end{aligned}$$

are valid for arbitrary $\tilde{z}_h, \tilde{u}_h \in V_h$ where $\hat{\rho}^* := \langle \lambda_{n,H} - \lambda_n, z_n \rangle + (\lambda_{t,H} - \lambda_t, sz_t)_{0, \Gamma_C}$.

Proof. Obviously, we have $R_u(u - u_h) = 0$ which gives us the first equation by Theorem 5.2. The linearity of J_u implies

$$J_u(u) - J_u(u_h) = J'_u(u) - J'_u(u_h) = a(u - u_h, z).$$

Consequently, the second equation directly follows from Lemma 5.1. □

The main result of Theorem 5.2 and Corollary 5.3 is that the same error representations as in the DWR approach for variational equations is obtained up to the contributions ρ^* and $\hat{\rho}^*$. Hence, existing implementations of the DWR method can easily be extended to frictional contact problems.

6. Error estimation of the displacement field and the Lagrange multipliers. In this section, we assume that the user-defined functional measures some quantities of physical interest in the displacement field and, additionally, in the Lagrange multipliers. It is denoted by $J : W \rightarrow \mathbb{R}$ with $W := V \times M_n \times M_t$, $M_n := H^{-1/2}(\Gamma_C)$ and $M_t := L^2(\Gamma_C)$. Again, we assume that J is (three times) Fréchet-differentiable where $J'_u : W \rightarrow V^*$, $J'_n : W \rightarrow M_n^* \simeq H^{1/2}(\Gamma_C)$ and $J'_t : W \rightarrow M_t^* \simeq M_t$ denote its derivatives with respect to V , M_n and M_t . To estimate $J(u, \lambda_n, \lambda_t) - J(u_h, \lambda_{n,H}, \lambda_{t,H})$ using the concept of dual weighted residual error estimations we extend the dual problem via the following mixed formulation: We seek $(z, \xi_n, \xi_t) \in W$ such that

$$\begin{aligned} a(v, z) + \langle \xi_n, v_n \rangle + (\xi_t, sv_t)_{0, \Gamma_C} &= \langle J'_u(u, \lambda_n, \lambda_t), v \rangle \\ \langle \mu_n, z_n \rangle &= \langle J'_n(u, \lambda_n, \lambda_t), \mu_n \rangle \\ (\mu_t, sz_t)_{0, \Gamma_C} &= \langle J'_t(u, \lambda_n, \lambda_t), \mu_t \rangle \end{aligned} \tag{6.1}$$

for all $(v, \mu_n, \mu_t) \in W$. An approximation is given by $(z_h, \xi_{n,H}, \xi_{t,H}) \in W_{hH} := V_h \times M_H \times M_H^{k-1}$ fulfilling

$$\begin{aligned} a(v_h, z_h) + \langle \xi_{n,H}, v_{h,n} \rangle + (\xi_{t,H}, sv_{h,t})_{0,\Gamma_C} &= \langle J'_u(u_h, \lambda_{n,H}, \lambda_{t,H}), v_h \rangle \\ \langle \mu_{n,H}, z_{n,h} \rangle &= \langle J'_n(u_h, \lambda_{n,H}, \lambda_{t,H}), \mu_{n,H} \rangle \\ (\mu_{t,H}, sz_{t,h})_{0,\Gamma_C} &= \langle J'_t(u_h, \lambda_{n,H}, \lambda_{t,H}), \mu_{t,H} \rangle \end{aligned} \quad (6.2)$$

for all $(v_h, \mu_{n,H}, \mu_{t,H}) \in W_{hH}$. Using standard arguments of mixed methods, cf., e.g., [4], the unique existence of the solutions $(z, \lambda_n, \lambda_t)$ and $(z_h, \lambda_{n,H}, \lambda_{t,H})$ of (6.1) and (6.2) are ensured.

Following again the basic idea of the DWR method we reuse the primal residual Res of the last section and define the dual residuals $\text{Res}^* : V \rightarrow V^*$, $\text{Res}_n : V \rightarrow M_n^* \simeq H^{1/2}(\Gamma_C)$ and $\text{Res}_t : V \rightarrow M_t^* \simeq M_t$ by

$$\begin{aligned} \langle \text{Res}^*(w), v \rangle &:= \langle J'_u(u_h, \lambda_{n,H}, \lambda_{t,H}), v \rangle - (\xi_{n,H}, v_n)_{0,\Gamma_C} - (\xi_{t,H}, sv_t)_{0,\Gamma_C} - a(v, w), \\ \langle \text{Res}_n^*(w), \mu_n \rangle &:= \langle J'_n(u_h, \lambda_{n,H}, \lambda_{t,H}), \mu_n \rangle - \langle \mu_n, w_n \rangle, \\ \langle \text{Res}_t^*(w), \mu_t \rangle &:= \langle J'_t(u_h, \lambda_{n,H}, \lambda_{t,H}), \mu_t \rangle - (\mu_t, sw_t)_{0,\Gamma_C}. \end{aligned}$$

Obviously, we have

$$\langle \text{Res}^*(z_h), v_h \rangle = \langle \text{Res}_n^*(z_h), \mu_{n,H} \rangle = \langle \text{Res}_t^*(z_h), \mu_{t,H} \rangle = 0 \quad (6.3)$$

for all $(v_h, \mu_{n,H}, \mu_{t,H}) \in W_{hH}$. Again, the fundamental theorem of calculus and the trapezoidal rule yield

$$\begin{aligned} &J(u, \lambda_n, \lambda_t) - J(u_h, \lambda_{n,H}, \lambda_{t,H}) \\ &= \int_0^1 \langle J'_u(u_\kappa, \lambda_{n,\kappa}, \lambda_{t,\kappa}), u - u_h \rangle + \langle J'_n(u_\kappa, \lambda_{n,\kappa}, \lambda_{t,\kappa}), \lambda_n - \lambda_{n,H} \rangle \\ &\quad + \langle J'_t(u_\kappa, \lambda_{n,\kappa}, \lambda_{t,\kappa}), \lambda_t - \lambda_{t,H} \rangle d\kappa \\ &= \frac{1}{2} (\langle J'_u(u, \lambda_n, \lambda_t), u - u_h \rangle + \langle J'_n(u, \lambda_n, \lambda_t), \lambda_n - \lambda_{n,H} \rangle + \langle J'_t(u, \lambda_n, \lambda_t), \lambda_t - \lambda_{t,H} \rangle) \\ &\quad + \langle J'_u(u_h, \lambda_{n,H}, \lambda_{t,H}), u - u_h \rangle + \langle J'_n(u_h, \lambda_{n,H}, \lambda_{t,H}), \lambda_n - \lambda_{n,H} \rangle \\ &\quad + \langle J'_t(u_h, \lambda_{n,H}, \lambda_{t,H}), \lambda_t - \lambda_{t,H} \rangle + R(u - u_h, \lambda_n - \lambda_{n,H}, \lambda_t - \lambda_{t,H}) \end{aligned} \quad (6.4)$$

with

$$(u_\kappa, \lambda_{n,\kappa}, \lambda_{t,\kappa}) := (u + \kappa(u - u_h), \lambda_n + \kappa(\lambda_n - \lambda_{n,H}), \lambda_t + \kappa(\lambda_t - \lambda_{t,H})),$$

and the remainder

$$R(v, \mu_n, \mu_t) := \frac{1}{2} \int_0^1 \langle \langle \langle J'''(u_\kappa, \lambda_{n,\kappa}, \lambda_{t,\kappa})(v, \mu_n, \mu_t) \rangle \rangle \rangle \kappa(\kappa - 1) d\kappa$$

where $J''' : W \rightarrow \mathcal{L}(W, \mathcal{L}(W, W^*))$ is the third derivative of J . Finally, we obtain the following error representation.

THEOREM 6.1. *The error representation*

$$\begin{aligned} &J(u, \lambda_n, \lambda_t) - J(u_h, \lambda_{n,H}, \lambda_{t,H}) \\ &= \frac{1}{2} \langle \text{Res}(u_h), z - \tilde{z}_h \rangle + \frac{1}{2} \langle \text{Res}^*(z_h), u - \tilde{u}_h \rangle + \frac{1}{2} \langle \text{Res}_n^*(z_h), \lambda_n - \tilde{\lambda}_{n,H} \rangle \\ &\quad + \frac{1}{2} \langle \text{Res}_t^*(z_h), \lambda_t - \tilde{\lambda}_{t,H} \rangle + \rho + R(u - u_h, \lambda_n - \lambda_{n,H}, \lambda_t - \lambda_{t,H}) \end{aligned}$$

holds for arbitrary $\tilde{z}_h, \tilde{u}_h \in V_h$, $\tilde{\lambda}_{n,H} \in M_H$ and $\tilde{\lambda}_{t,H} \in (M_H)^{k-1}$ where

$$\rho := \left\langle \frac{1}{2}(\xi_n + \xi_{n,H}), u_n - u_{h,n} \right\rangle + \left\langle \frac{1}{2}(\xi_t + \xi_{t,H}), s(u_t - u_{h,t}) \right\rangle_{0,\Gamma_C}.$$

Proof. With $e := u - u_h$, $e_n^\lambda := \lambda_n - \lambda_{n,H}$ and $e_t^\lambda := \lambda_t - \lambda_{t,H}$, we obtain by Lemma 5.1 and 4.1 as well as (6.3)

$$\begin{aligned} & a(e, z) + \langle \xi_n, e_n \rangle + (\xi_t, se_t)_{0,\Gamma_C} + \langle e_n^\lambda, z_n \rangle + (e_t^\lambda, sz_t)_{0,\Gamma_C} \\ & + \langle J'_u(u_h, \lambda_{n,H}, \lambda_{t,H}), e \rangle + \langle J'_n(u_h, \lambda_{n,H}, \lambda_{t,H}), e_n^\lambda \rangle + \langle J'_t(u_h, \lambda_{n,H}, \lambda_{t,H}), e_t^\lambda \rangle \\ = & \langle \text{Res}(u_h), z - \tilde{z}_h \rangle + \langle J'_u(u_h, \lambda_{n,H}, \lambda_{t,H}), e \rangle - \langle \xi_{n,H}, e_n \rangle - (\xi_{t,H}, se_t)_{0,\Gamma_C} - a(e, z_h) \\ & + \langle J'_n(u_h, \lambda_{n,H}, \lambda_{t,H}), e_n^\lambda \rangle - \langle e_n^\lambda, z_{h,n} \rangle + \langle J'_t(u_h, \lambda_{n,H}, \lambda_{t,H}), e_t^\lambda \rangle - (e_t^\lambda, z_{h,t})_{0,\Gamma_C} \\ & + \langle \xi_n + \xi_{n,H}, e_n \rangle + (\xi_t + \xi_{t,H}, se_t)_{0,\Gamma_C} \\ = & \langle \text{Res}(u_h), z - \tilde{z}_h \rangle + \langle \text{Res}^*(z_h), u - u_h \rangle \\ & + \langle \text{Res}_n^*(z_h), \lambda_n - \lambda_{n,H} \rangle + \langle \text{Res}_t^*(z_h; \cdot), \lambda_t - \lambda_{t,H} \rangle + 2\rho \\ = & \langle \text{Res}(u_h), z - \tilde{z}_h \rangle + \langle \text{Res}^*(z_h), u - \tilde{u}_h \rangle \\ & + \langle \text{Res}_n^*(z_h), \lambda_n - \tilde{\lambda}_{n,H} \rangle + \langle \text{Res}_t^*(z_h; \cdot), \lambda_t - \tilde{\lambda}_{t,H} \rangle + 2\rho. \end{aligned}$$

Using (6.4) and the calculation above, we conclude

$$\begin{aligned} & J(u) - J(u_h) \\ = & \frac{1}{2}(\langle J'_u(u, \lambda_n, \lambda_t), e \rangle + \langle J'_n(u, \lambda_n, \lambda_t), e_n^\lambda \rangle + \langle J'_t(u, \lambda_n, \lambda_t), e_t^\lambda \rangle \\ & + \langle J'_u(u_h, \lambda_{n,H}, \lambda_{t,H}), e \rangle + \langle J'_n(u_h, \lambda_{n,H}, \lambda_{t,H}), e_n^\lambda \rangle + \langle J'_t(u_h, \lambda_{n,H}, \lambda_{t,H}), e_t^\lambda \rangle) \\ & + R(e, e_n^\lambda, e_t^\lambda) \\ = & \frac{1}{2}(a(e, z) + \langle \xi_n, e_n \rangle + (\xi_t, se_t)_{0,\Gamma_C} + \langle e_n^\lambda, z_n \rangle + (e_t^\lambda, sz_t)_{0,\Gamma_C} \\ & + \langle J'_u(u_h, \lambda_{n,H}, \lambda_{t,H}), e \rangle + \langle J'_n(u_h, \lambda_{n,H}, \lambda_{t,H}), e_n^\lambda \rangle + \langle J'_t(u_h, \lambda_{n,H}, \lambda_{t,H}), e_t^\lambda \rangle) \\ & + R(e, e_n^\lambda, e_t^\lambda) \\ = & \frac{1}{2}\langle \text{Res}(u_h), z - \tilde{z}_h \rangle + \frac{1}{2}\langle \text{Res}^*(z_h), u - \tilde{u}_h \rangle \\ & + \frac{1}{2}\langle \text{Res}_n^*(z_h), \lambda_n - \tilde{\lambda}_{n,H} \rangle + \frac{1}{2}\langle \text{Res}_t^*(z_h), \lambda_t - \tilde{\lambda}_{t,H} \rangle + \rho + R(e, e_n^\lambda, e_t^\lambda). \end{aligned}$$

□

Again, if J is linear, some simplifications can be done.

COROLLARY 6.2. *If $J(v, \mu_n, \mu_t) = J_u(v) + J_n(\mu_n) + J_t(\mu_t)$ with $J_u \in V^*$, $J_n \in M_n^*$ and $J_t \in M_t^*$ the identities*

$$\begin{aligned} & J(u, \lambda_n, \lambda_t) - J(u_h, \lambda_{n,H}, \lambda_{t,H}) = \langle \text{Res}(u_h), z - \tilde{z}_h \rangle + \hat{\rho} \\ = & \frac{1}{2}\langle \text{Res}(u_h), z - \tilde{z}_h \rangle + \frac{1}{2}\langle \text{Res}^*(z_h), u - \tilde{u}_h \rangle \\ & + \frac{1}{2}\langle \text{Res}_n^*(z_h), \lambda_n - \tilde{\lambda}_{n,H} \rangle + \frac{1}{2}\langle \text{Res}_t^*(z_h), \lambda_t - \tilde{\lambda}_{t,H} \rangle + \rho \end{aligned}$$

are fulfilled for arbitrary $\tilde{z}_h, \tilde{u}_h \in V_h$, $\tilde{\lambda}_{n,H} \in M_H$ and $\tilde{\lambda}_{t,H} \in (M_H)^{k-1}$ where $\hat{\rho} := \langle \xi_{n,H}, u_n - u_{h,n} \rangle + \langle \xi_{t,H}, s(u_t - u_{h,t}) \rangle_{0,\Gamma_C}$.

Proof. Obviously, we have $R(e, e_n^\lambda, e_t^\lambda) = 0$ which gives us the second equation by Theorem 6.1. Because of the linearity of J_u , J_n and J_t , we have $J'_u(u) = J'_u(u_h)$, $J'_n(\lambda_n) = J'_n(\lambda_{n,H})$ and $J'_t(\lambda_t) = J'_t(\lambda_{t,H})$. Thus, we obtain from Lemma 4.1 and (6.3)

$$\begin{aligned}
\langle \text{Res}(u_h), z - \tilde{z}_h \rangle &= \langle \text{Res}(u_h), z \rangle \\
&= \ell(z) - (\lambda_n, z_n)_{0,\Gamma_C} - (\lambda_t, sz_t)_{0,\Gamma_C} - a(u_h, z) \\
&\quad + (\lambda_n - \lambda_{n,H}, z_n)_{0,\Gamma_C} + (\lambda_t - \lambda_{t,H}, sz_t)_{0,\Gamma_C} \\
&= a(e, z) + \langle J'_n(\lambda_n), e_n^\lambda \rangle + \langle J'_t(\lambda_t), e_t^\lambda \rangle \\
&= \langle J'_u(u), e \rangle - \langle \xi_n, e_n \rangle - \langle \xi_t, se_t \rangle_{0,\Gamma_C} + \langle J'_n(\lambda_n), e_n^\lambda \rangle + \langle J'_t(\lambda_t), e_t^\lambda \rangle \\
&= \langle J'_u(u_h), e \rangle - \langle \xi_{n,H}, e_n \rangle - \langle \xi_{t,H}, se_t \rangle_{0,\Gamma_C} - a(e, z_h) + \langle J'_n(\lambda_{n,H}), e_n^\lambda \rangle - \langle e_n^\lambda, z_{h,n} \rangle \\
&\quad + \langle J'_t(\lambda_{t,H}), e_t^\lambda \rangle - (e_t^\lambda, sz_{h,t})_{0,\Gamma_C} + \langle \xi_{n,H} - \xi_n, e_n \rangle + \langle \xi_{t,H} - \xi_t, se_t \rangle_{0,\Gamma_C} \\
&= \langle \text{Res}^*(z_h), e \rangle + \langle \text{Res}_n^*(z_h), e_n^\lambda \rangle + \langle \text{Res}_t^*(z_h), e_t^\lambda \rangle + 2\hat{\rho} - 2\rho \\
&= \langle \text{Res}^*(z_h), u - \tilde{u}_h \rangle + \langle \text{Res}_n^*(z_h), \lambda_n - \tilde{\lambda}_{n,H} \rangle + \langle \text{Res}_t^*(z_h), \lambda_t - \tilde{\lambda}_{t,H} \rangle + 2\hat{\rho} - 2\rho.
\end{aligned}$$

□

As in Section 5, we again obtain the same error representations as for the DWR method for variational equations. Only, the error contribution ρ (or $\hat{\rho}$) has to be added.

7. Evaluation and Localization. To evaluate the error representations of the Theorems 5.2 and 6.1 we omit the remainder as it is of higher order and, moreover, approximate the unknowns u , z , λ_n , λ_t , ξ_n and ξ_t using higher-order and averaging interpolations. To approximate the primal and dual solutions u and z we determine quadratic interpolations on a coarser mesh element. This, however, requires a special structure of the adaptively refined finite element mesh, cf. Figure 7.1. This so-called patch-structure is obtained through the refinement of all sons of a refined element, provided that one of these sons is actually marked for refinement. A quadratic interpolation $I(\tilde{z}_h)$ of $\tilde{z}_h \in V_h$ on the coarser mesh element is then componentwisely calculated by the nodal values of $\tilde{z}_{h,i}$ on the fine mesh elements. We refer to [1] for more details and alternativ choices for the interpolation.

For the Lagrange multipliers λ_n and λ_t as well as the dual solutions ξ_n and ξ_t , we make use of standard averaging interpolations $A_n(\mu_{n,H})$ and $A_t(\mu_{t,H})$ which are (componentwisely) defined as the linear interpolant of the values $(\sum_{E \in \mathcal{M}(x)} |E|)^{-1} \sum_{E \in \mathcal{M}(x)} \mu_H|E$ in a grid node x where $\mu_H \in M_H$ and $\mathcal{M}(x) := \{E \in \mathcal{E}_C \mid x \in \bar{E}\}$.

Using I , A_n and A_t we finally obtain from Theorem 5.2

$$J_u(u) - J_u(u_h) \approx \frac{1}{2} \langle \text{Res}(u_h), I(z_h) - z_h \rangle + \frac{1}{2} \langle \text{Res}_u^*(z_h), I(u_h) - u_h \rangle + \tilde{\rho}^*$$

with

$$\begin{aligned}
\tilde{\rho}^* &:= (\lambda_{n,H} - A_n(\lambda_{n,H}), \frac{1}{2}(I(z_h)_n + z_{h,n}))_{0,\Gamma_C} \\
&\quad + (\lambda_{t,H} - A_t(\lambda_{t,H}), s \frac{1}{2}(I(z_h)_t + z_{h,t}))_{0,\Gamma_C}.
\end{aligned}$$

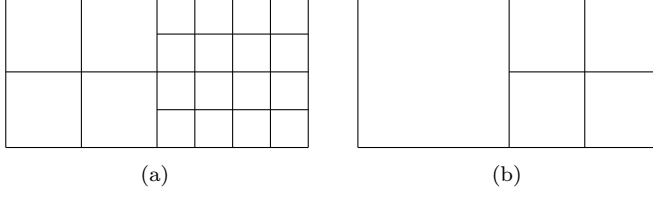


FIG. 7.1. (a) Mesh with patch structure, (b) coarser mesh

From Theorem 6.1, we get

$$\begin{aligned}
& J(u, \lambda_n, \lambda_t) - J(u_h, \lambda_{n,H}, \lambda_{t,H}) \\
& \approx \frac{1}{2} \langle \text{Res}(u_h), I(z_h) - z_h \rangle + \frac{1}{2} \langle \text{Res}^*(z_h), I(u_h) - u_h \rangle \\
& \quad + \frac{1}{2} \langle \text{Res}_n^*(z_h), A_n(\lambda_{n,H}) - \lambda_{n,H} \rangle + \frac{1}{2} \langle \text{Res}_t^*(z_h), A_t(\lambda_{t,H}) - \lambda_{t,H} \rangle + \tilde{\rho}
\end{aligned}$$

with

$$\begin{aligned}
\tilde{\rho} := & \left(\frac{1}{2} (A_n(\xi_{n,H}) + \xi_{n,H}), I(u_h)_n - u_{h,n} \right)_{0, \Gamma_C} \\
& + \left(\frac{1}{2} (A_t(\xi_{t,H}) + \xi_{t,H}), s(I(u_h)_t - u_{h,t}) \right)_{0, \Gamma_C}.
\end{aligned}$$

REMARK 7.1. The quadratic interpolation $I(\tilde{z}_h)$ is not continuous on meshes with hanging nodes. To define a continuous interpolation, one has to include additional constraints on irregular edges (or faces), cf. [15].

For the use of the error representation within an adaptive scheme, we have to localize the error contributions given by the primal and dual residuals Res , Res_u^* , Res^* , Res_n^* and Res_t^* as well as the additional terms $\tilde{\rho}$ and $\tilde{\rho}^*$ with respect to the mesh elements. The error localization regarding to Res , Res_u^* and Res^* may be done by integration by parts. In this case the primal residual Res is given by

$$\langle \text{Res}(w), v \rangle = \sum_{T \in \mathcal{T}} (\langle \text{Res}_T(w), v \rangle + \sum_{E \in \mathcal{E}_T} \langle \text{Res}_E(w), v \rangle) \quad (7.1)$$

with the primal local residuals $\text{Res}_T, \text{Res}_E : V \rightarrow V^*$, $T \in \mathcal{T}$, $E \in \mathcal{E}^\circ \cup \mathcal{E}_C \cup \mathcal{E}_N$,

$$\langle \text{Res}_T(w), v \rangle := (f + \text{div } \sigma(w), v)_{0, T}$$

$$\langle \text{Res}_E(w), v \rangle := \begin{cases} \frac{1}{2} ([\sigma_{n_E}(w)], v)_{0, E}, & E \in \mathcal{E}^\circ, \\ (-\lambda_{n,H} - \sigma_{n_E, n_E}(w), v_{n_E})_{0, E} \\ \quad + (-\lambda_{t,H} - \sigma_{n_E, t_E}(w), s v_{t_E})_{0, E}, & E \in \mathcal{E}_C, \\ (b - \sigma_{n_E}(w), v_N)_{0, E}, & E \in \mathcal{E}_N, \\ 0, & \text{else} \end{cases}$$

where \mathcal{E}° contains the internal edges (or faces), \mathcal{E}_N the edges (or faces) on Γ_N and \mathcal{E}_T the edges (or faces) of $T \in \mathcal{T}$. The vector n_E denotes a unit vector orthogonal to $E \in \mathcal{E}$. It indicates the outer normal vector if $E \in \mathcal{E}_C \cup \mathcal{E}_N$. The vector t_E is a tangential vector of $E \in \mathcal{E}_C \cup \mathcal{E}_N$.

Assuming that the error functional J_u is given by $J_u(v) = \int_{\Omega} j(x, v(x)) dx$ with some possibly non-linear function $j : \mathbb{R}^k \times \mathbb{R}^k \rightarrow \mathbb{R}$, the dual residual is

$$\langle \text{Res}_u^*(w), v \rangle = \sum_{T \in \mathcal{T}} (\langle \text{Res}_T^*(w), v \rangle) + \sum_{E \in \mathcal{E}_T} \langle \text{Res}_{u,E}^*(w), v \rangle$$

where the dual local residuals are defined as $\langle \text{Res}_T^*(w), v \rangle := (j' + \text{div } \sigma(w), v)_{0,T}$ with $j'(x) := \frac{\partial j}{\partial v}(x, u_h(x))$ and

$$\langle \text{Res}_{u,E}^*(w), v \rangle := \begin{cases} \frac{1}{2}([\sigma_{n_E}(w)], v)_{0,E}, & E \in \mathcal{E}^\circ, \\ (-\sigma_{n_E}(w), v_N)_{0,E}, & E \in \mathcal{E}_N, \\ 0, & \text{else.} \end{cases}$$

Provided that the error functional J is given as

$$J(v, \mu_n, \mu_t) = J_u(v) + \int_{\Gamma_C} j_C(x, v_C(x), \mu_n(x), \mu_t(x)) dx$$

with the (non-linear) function $j_C : \mathbb{R}^k \times \mathbb{R}^k \times \mathbb{R} \times \mathbb{R}^{k-1} \rightarrow \mathbb{R}$ we obtain

$$\langle \text{Res}^*(w), v \rangle = \sum_{T \in \mathcal{T}} (\langle \text{Res}_T^*(w), v \rangle) + \sum_{E \in \mathcal{E}_T} \langle \text{Res}_E^*(w), v \rangle$$

with

$$\langle \text{Res}_E^*(w), v \rangle := \begin{cases} \langle \text{Res}_{u,E}^*(w), v \rangle, & E \in \mathcal{E}^\circ \cup \mathcal{E}_N, \\ (j'_{C,u,n} - \xi_{n,H} - \sigma_{n_E, n_E}(w), v_n) \\ \quad + (j'_{C,u,t} - \xi_{t,H} - \sigma_{n_E, n_t}(w), v_t)_{0,E}, & E \in \mathcal{E}_C, \\ 0, & \text{else} \end{cases}$$

and $j'_{C,u}(x) := \frac{\partial j_C}{\partial v_C}(x, u_{h,N}(x), \lambda_{n,H}(x), \lambda_{t,H}(x))$, $x \in \Gamma_C$. The residuals Res_l^* , $l \in \{n, t\}$, are given as follows

$$\langle \text{Res}_l^*(w), \mu_l \rangle := \sum_{T \in \mathcal{T}} \sum_{E \in \mathcal{E}_T} \langle \text{Res}_{l,E}^*(w), \mu_l \rangle$$

with $\text{Res}_l^*(w), \mu_l := (j'_{C,l} - \mu_l, w_l)_{0,E}$ for $E \in \mathcal{E}_C$ and 0 otherwise as well as $j'_{C,l}(x) := \frac{\partial j_C}{\partial \mu_l}(x, u_{h,N}(x), \lambda_{n,H}(x), \lambda_{t,H}(x))$, $x \in \Gamma_C$. Moreover, we define for $E \in \mathcal{E}_C$

$$\begin{aligned} \tilde{\rho}_E^* &:= \begin{cases} (\lambda_{n,H} - A_n(\lambda_{n,H}), \frac{1}{2}(I(z_h)_n + z_{h,n}))_{0,E} \\ \quad + (\lambda_{t,H} - A_t(\lambda_{t,H}), s \frac{1}{2}(I(z_h)_t + z_{h,t}))_{0,E}, \end{cases} \\ \tilde{\rho}_E &:= \begin{cases} (\frac{1}{2}(A_n(\xi_{n,H}) + \xi_{n,H}), I(u_h)_n - u_{h,n})_{0,E} \\ \quad + (\frac{1}{2}(A_t(\xi_{t,H}) + \xi_{t,H}), s(I(u_h)_t - u_{h,t}))_{0,E}, \end{cases} \end{aligned}$$

and $\tilde{\rho}_E^* = \tilde{\rho}_E = 0$ for $E \notin \mathcal{E}_C$. Eventually, the error contributions are then given by

$$\begin{aligned} \eta_T &:= \frac{1}{2} (\langle \text{Res}_T(u_h), I(z_h) - z_h \rangle + \sum_{E \in \mathcal{E}_T} \langle \text{Res}_E(u_h), I(z_h) - z_h \rangle) \\ \eta_{u,T}^* &:= \frac{1}{2} (\langle \text{Res}_T^*(z_h), I(u_h) - u_h \rangle + \sum_{E \in \mathcal{E}_T} \langle \text{Res}_{u,E}^*(z_h), I(u_h) - u_h \rangle) \\ \eta_T^* &:= \frac{1}{2} (\langle \text{Res}_T^*(z_h), I(u_h) - u_h \rangle + \sum_{E \in \mathcal{E}_T} \langle \text{Res}_E^*(z_h), I(u_h) - u_h \rangle) \\ \eta_{l,T}^* &:= \frac{1}{2} \left(\sum_{E \in \mathcal{E}_T} \langle \text{Res}_{l,E}^*(z_h), A_l(\mu_{l,H}) - \mu_{l,H} \rangle \right), \quad l \in \{n, t\} \\ \tilde{\rho}_T^* &:= \sum_{E \in \mathcal{E}_T} \tilde{\rho}_E^*, \quad \tilde{\rho}_T := \sum_{E \in \mathcal{E}_T} \tilde{\rho}_E, \quad \tilde{\rho}^* = \sum_{T \in \mathcal{T}} \tilde{\rho}_T^*, \quad \tilde{\rho} = \sum_{T \in \mathcal{T}} \tilde{\rho}_T, \end{aligned} \quad (7.2)$$

$$\bar{\eta}_u := \sum_{T \in \mathcal{T}} (\eta_T + \eta_{u,T}^*), \quad \bar{\eta} := \sum_{T \in \mathcal{T}} (\eta_T + \eta_T^* + \eta_{n,T}^* + \eta_{t,T}^*), \quad (7.3)$$

and the localized error estimations by

$$J_u(u) - J_u(u_h) \approx \eta_u := \bar{\eta}_u + \tilde{\rho}^* \quad (7.4)$$

$$J(u, \lambda_n, \lambda_t) - J(u_h, \lambda_{n,H}, \lambda_{t,H}) \approx \eta := \bar{\eta} + \tilde{\rho}. \quad (7.5)$$

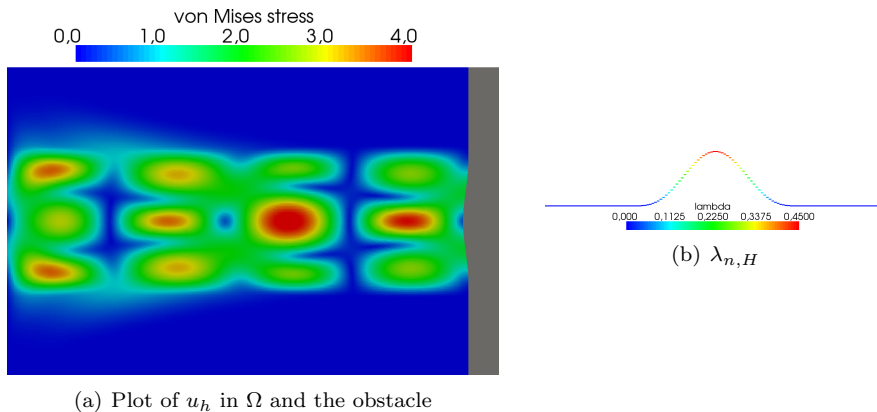
REMARK 7.2. The use of integration by parts to localize the error contributions lead to a significant implementational effort since jumps across edges or faces have to be calculated and, moreover, the evaluation of the (possibly nonlinear) operator of the strong formulation could also be very involved. An alternative localization technique avoiding these difficulties is proposed in [3].

8. Numerical results. In this section, we consider several numerical examples to show the applicability of the theoretical findings. The first one is a frictionless 2D Signorini problem, where $\Omega := [-3, 0] \times [-1, 1]$. We prescribe homogeneous Dirichlet boundary conditions on $\Gamma_D := \{-3\} \times [-1, 1]$ and homogeneous Neumann boundary conditions on $\Gamma_N := (-3, 0) \times \{-1, 1\}$. The contact boundary is $\Gamma_C := \{0\} \times [-1, 1]$. We consider Hooke's law with Young's modulus $E := 10$ and Poisson number $\nu := 0.3$ using the plain strain assumption. By L we denote the number of uniform refinements based on a coarse initial triangulation. To test the accuracy of the error estimators, we consider an example with the known solution $u(x, y) := (u_1(x, y), u_2(x, y))^T$, where

$$\begin{aligned} u_1(x, y) &:= \begin{cases} -(x+3)^2(y - \frac{x^2}{18} - \frac{1}{2})^4(y + \frac{x^2}{18} + \frac{1}{2})^4, & |y| < \frac{x^2}{18} + \frac{1}{2}, \\ 0, & \text{else,} \end{cases} \\ u_2(x, y) &:= \begin{cases} \frac{27}{\pi} \sin\left(\frac{4\pi(x+3)}{3}\right) [(y - \frac{1}{2})^3(y + \frac{1}{2})^4 + (y - \frac{1}{2})^4(y + \frac{1}{2})^3], & |y| < \frac{1}{2}, \\ 0, & \text{else.} \end{cases} \end{aligned}$$

The volume force is chosen as $f := -\text{div}(\sigma(u))$ and the obstacle as $g(y) := u_1(0, y)$. The discrete solution u_h is outlined in Figure 8.1, where M_Ω denotes the number of mesh elements and M_C the number of contact elements. First, we consider the quantity of interest

$$J_{a,1}(u) := \int_{B_{a,1}} \|u\|^2 dx, \quad B_{a,1} = [-1.5, -0.5] \times [-0.5, 0.5].$$

FIG. 8.1. Numerical solution of the first 2D example for $M_\Omega = 24576$ and $M_C = 64$

M_Ω	L	$I_{\text{eff}}(\eta)$	$I_{\text{eff}}(\tilde{\eta})$	$I_{\text{eff}}(\eta_u)$	$I_{\text{eff}}(\tilde{\eta}_u)$
96	0	3.809	7.073	6.332	5.669
384	1	0.611	0.636	0.617	0.599
1536	2	0.966	0.992	0.961	0.939
6144	3	0.984	1.008	0.976	0.955
24576	4	0.979	1.002	0.969	0.949
98304	5	0.977	0.999	0.967	0.946
393216	6	0.976	0.999	0.9666	0.946

TABLE 8.1

Effectivity indices for different error estimators w.r.t. $J_{a,1}$

In particular, we study the relative discretization error E_{rel} and the effectivity index $I_{\text{eff}}(\tilde{\eta})$ for a quantity of interest J and an error estimator $\tilde{\eta}$. The quantities E_{rel} and $I_{\text{eff}}(\tilde{\eta})$ are defined by

$$E_{\text{rel}} := \frac{|J(u, \lambda_n, \lambda_t) - J(u_h, \lambda_{n,H}, \lambda_{t,H})|}{|J(u, \lambda_n, \lambda_t)|},$$

and

$$I_{\text{eff}}(\tilde{\eta}) := \frac{J(u, \lambda_n, \lambda_t) - J(u_h, \lambda_{n,H}, \lambda_{t,H})}{\tilde{\eta}}.$$

In Table 8.1, effectivity indices for the presented error estimators η , $\tilde{\eta}$, η_u , and $\tilde{\eta}_u$ from (7.3) and (7.4)-(7.5) are compared. We observe that all four estimators lead to accurate estimates of the error w.r.t. $J_{a,1}$. We would expect that η yields the most accurate estimates. But this is not the case, since $\tilde{\eta}$ seems to be more accurate. Moreover, the effectivity indices do not converge to 1 exactly. To study these phenomena in more detail, we consider quantities of interest, where the solution of the corresponding dual problem is known, so that the individual contributions to the error estimators can be calculated exactly. We choose the quantity of interest $J_{a,2}(u) := \int_\Omega -\text{div}(\sigma(\bar{z})) \cdot u \, dx$. The solution $\bar{z}(x, y) = 0.1(\bar{z}_1(x, y), \bar{z}_2(x, y))^T$ of the

M_Ω	L	$I_{\text{eff}}(\eta_u)$	$I_{\text{eff}}(\bar{\eta}_u)$	$A_{\text{eff}}(\bar{\eta}_u)$	$A_{\text{eff}}(\rho^*)$
96	0	5.652	5.256	4.987	3.829
384	1	0.903	0.877	0.995	4.128
1536	2	0.951	0.923	0.998	2.539
6144	3	0.964	0.935	0.999	2.173
24576	4	0.965	0.936	1.000	2.154
98304	5	0.965	0.936	1.000	2.155
393216	6	0.965	0.936	1.000	2.155

TABLE 8.2

Effectivity indices for η_u w.r.t. $J_{a,2}$

M_Ω	L	$I_{\text{eff}}(\eta)$	$I_{\text{eff}}(\bar{\eta})$	$A_{\text{eff}}(\bar{\eta})$	$A_{\text{eff}}(\rho)$
96	0	1.551	1.121	1.247	0.453
384	1	2.034	1.825	1.053	7.527
1536	2	1.221	1.118	1.014	1.226
6144	3	1.099	1.011	1.005	0.081
24576	4	1.088	1.002	1.002	$8.44 \cdot 10^{-4}$
98304	5	1.086	1.001	1.001	$7.76 \cdot 10^{-4}$
393216	6	1.086	1.000	1.000	$7.71 \cdot 10^{-4}$

TABLE 8.3

Effectivity indices for η w.r.t. $J_{a,3}$

dual problem is given by

$$\begin{aligned}\bar{z}_1(x, y) &:= \left[\frac{1}{4} + \frac{65}{144}x^2 + \frac{11}{144}x^3 - \frac{1}{36}x^4 \right] (1 - y^2)^3, \\ \bar{z}_2(x, y) &:= \left[x + \frac{7}{12}x^2 + \frac{1}{3}x^3 + \frac{1}{12}x^4 \right] \frac{3}{2}y(1 - y^2)^2.\end{aligned}$$

To study the influence of the individual contributions on $\bar{\eta}_u$, we define

$$\begin{aligned}A_{\text{eff}}(\bar{\eta}_u) &:= (\langle \text{Res}(u_h), \bar{z} - \tilde{z}_h \rangle + \langle \text{Res}_u^*(z_h), u - \tilde{u}_h \rangle) / 2\bar{\eta}_u, \\ A_{\text{eff}}(\rho^*) &:= \rho^* / \tilde{\rho}^*,\end{aligned}$$

with ρ^* and $\tilde{\rho}^*$ from (7.2). In Table 8.2, the accuracy of the different parts of the estimator η_u are compared. Obviously, $A_{\text{eff}}(\bar{\eta}_u)$ converges towards 1. Consequently the approximation of the residuals is asymptotically exact. The additional term ρ^* is not computed asymptotically exactly. As shown in Table 8.2, ρ^* is underestimated by $\tilde{\rho}^*$ with a asymptotically constant factor of 2.155. Thus, $\tilde{\rho}^*$ is of the same order in h as ρ^* . The reason for the asymptotical inexactness may, therefore, lie in the approximation of ρ^* by $\tilde{\rho}^*$. It should be noted that the additional term ρ^* is about a factor 10 smaller than the residuals, so that the underestimation has no essential effect on the overall estimation. To study η in more detail, the slightly modified analytical dual solution $z(x, y) = 0.1(z_1(x, y), \bar{z}_2(x, y))^\top$, with

$$z_1(x, y) := \left[\frac{3}{4}x^2 + \frac{1}{4}x^3 \right] (1 - y^2)^3,$$

and $\xi_n(y) := \sigma(z(0, y))_n$ is chosen. The quantity of interest is given as above by

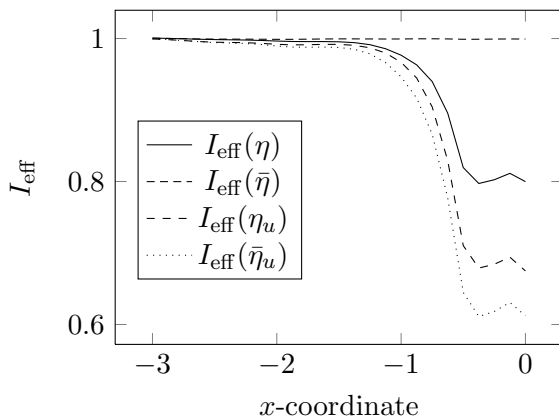


FIG. 8.2. Effectivity indices for different error estimators w.r.t. $J_{a,x}$ for $M_\Omega = 98304$

$J_{a,3}(u) := \int_\Omega -\operatorname{div}(\sigma(z)) \cdot u \, dx$. We define

$$A_{\text{eff}}(\bar{\eta}) := \left(\langle \operatorname{Res}(u_h), z - \tilde{z}_h \rangle + \langle \operatorname{Res}^*(z_h), u - \tilde{u}_h \rangle + \langle \operatorname{Res}_n^*(z_h), \lambda_n - \tilde{\lambda}_{n,H} \rangle \right) / 2\bar{\eta},$$

$$A_{\text{eff}}(\rho) := \rho / \tilde{\rho}.$$

In Table 8.3, the different indicators for the accuracy of the estimator η are compared. We observe that $A_{\text{eff}}(\bar{\eta})$ converges towards 1, i.e. the residual terms are asymptotically exactly resolved. The extra term ρ is overestimated by a factor of 1250, which is asymptotically constant. Hence, $\tilde{\rho}$ and ρ are of the same order in h . Since ρ is about a factor 10000 smaller than the residuals, the estimate based on $\bar{\eta}$, where ρ is neglected, is more accurate than the one using η including $\tilde{\rho}$, see Table 8.1 and 8.3.

To examine the influence of the quantity of interest on the effectivity indices w.r.t. η , $\bar{\eta}$, η_u , and $\bar{\eta}_u$, we consider

$$J_{a,x} := \int_{B_x} \|u\|^2 \, dx, \quad B_x = [x - 0.5, x + 0.5] \times [-0.5, 0.5]$$

for $x \in [-3, 0]$. In Figure 8.2, the behavior of the effectivity indices of η , $\bar{\eta}$, η_u , and $\bar{\eta}_u$ w.r.t. x is depicted. The estimator $\bar{\eta}$ leads to the best results, $I_{\text{eff}}(\bar{\eta}) \approx 1$ for all $x \in [-3, 0]$, due to the fact that for all $x \in [-3, 0]$ the extra term ρ is much smaller than the residual terms. The overestimation of ρ by $\tilde{\rho}$ leads to the poor accuracy of η , especially for values of x close to zero. The estimation by $\bar{\eta}_u$ is worse for x close to zero, since the additional term ρ^* becomes dominant. Even the estimator η_u leads only to minor improvements, since $\tilde{\rho}^*$ is approximating ρ^* not accurate enough.

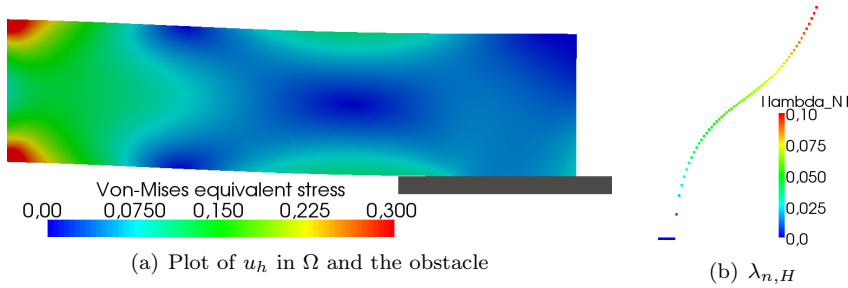
We now consider a quantity of interest, which depends on the Lagrange multiplier λ_n :

$$J_{a,4}(\lambda_n) := \int_{-0.125}^{0.375} \lambda_n^2(y) \, dy.$$

In Table 8.4, we observe that the use of $J_{a,4}$ leads to the same behaviour as the other quantities of interest. The term $\tilde{\rho}$ overestimates ρ and thus η is not as accurate as $\bar{\eta}$. Also here, the additional term ρ is considerably smaller than the residuals.

M_Ω	L	$I_{\text{eff}}(\eta)$	$I_{\text{eff}}(\bar{\eta})$
96	0	48.09	12.18
384	1	0.218	0.135
1536	2	1.216	0.839
6144	3	1.353	0.953
24576	4	1.389	0.984
98304	5	1.393	0.990
393216	6	1.393	0.991

TABLE 8.4

Effectivity indices for η w.r.t. $J_{a,4}$ FIG. 8.3. Numerical solution of the second 2D example for $M_\Omega = 65536$ and $M_C = 64$

In the second example, we study the influence of the error estimators on the discretization error, when they are within adaptive refinement algorithms. For this purpose, we set $\Omega := [0, 0.05] \times [0, 0.2]$, $\Gamma_D := [0, 0.05] \times \{0\}$, $\Gamma_C := \{0.05\} \times [0.15, 0.2]$, and $\Gamma_N := \partial\Omega \setminus (\Gamma_C \cup \Gamma_D)$. Furthermore, Hooke's law with plain stress, modulus of elasticity $E = 10$, and Poisson ratio $\nu = 0.33$ is used. The constant volume force is given by $f := (0.5, 0)^\top$ and the gap function by $g = 0.005$. The numerical solution is depicted in Figure 8.3, where the von-Mises equivalent stress

$$\sigma_{M,2}(\sigma, \sigma_e) := \frac{\sqrt{\sigma_{11}^2 + \sigma_{22}^2 + 3\sigma_{21}^2}}{\sigma_e}$$

with $\sigma_e = 1$ is depicted. We observe stress peaks in the left corners of the domain, where the Dirichlet boundary conditions change to Neumann boundary conditions. As quantity of interest, we consider $J(u) := \int_B \nabla u : \nabla u \, dx$ with $B = [0, 0.05]^2$.

In Figure 8.4, the meshes created in the 5th iteration of the adaptive algorithm based on a fixed fraction refinement strategy with refinement fraction 0.2 are shown. In the case that the error estimator $\bar{\eta}_u$ is used, adaptive refinements are only observed in the left part of the domain and, in particular, no additional refinements in the contact zone are done, see Figure 8.4(a). In contrast to this, the estimator η_u leads to refinements at the left end of the domain and also to strong adaptive refinements in the contact zone. The other parts of the domain are not refined, see Figure 8.4(b). The adaptive meshes based on $\bar{\eta}$ and η are very similar, they exhibit strong adaptive refinements in the left part of the domain and at the left end of the contact zone. We observe refinements in further parts of the domain, see Figure 8.4(c) and 8.4(d). The characteristics of the adaptive meshes remain in further sweeps of the adaptive algorithm. The relative error E_{rel} resulting from the adaptive schemes based on the

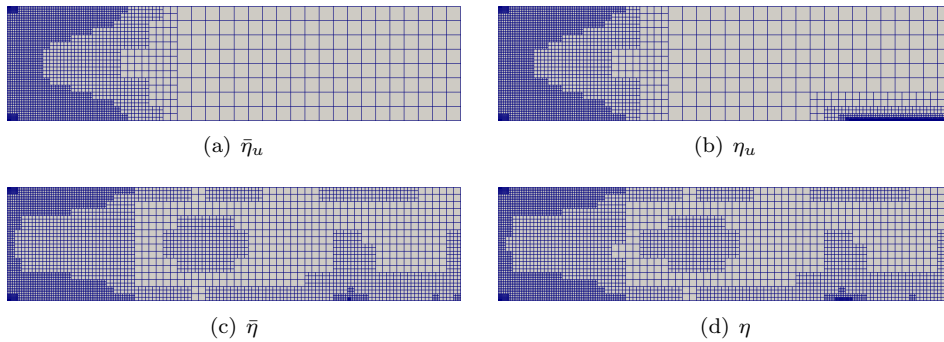


FIG. 8.4. Adaptive meshes based on different error estimators in the 5th iteration of the adaptive algorithm

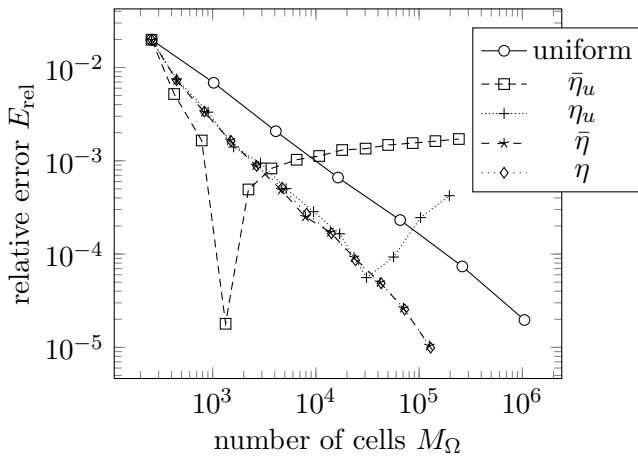
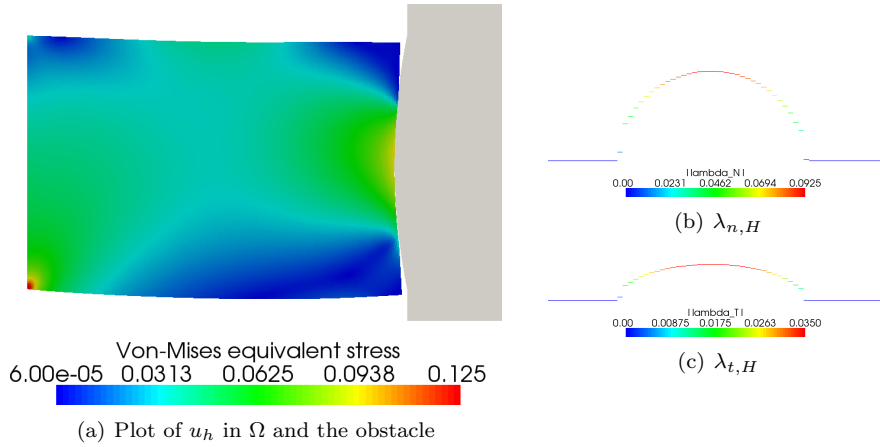
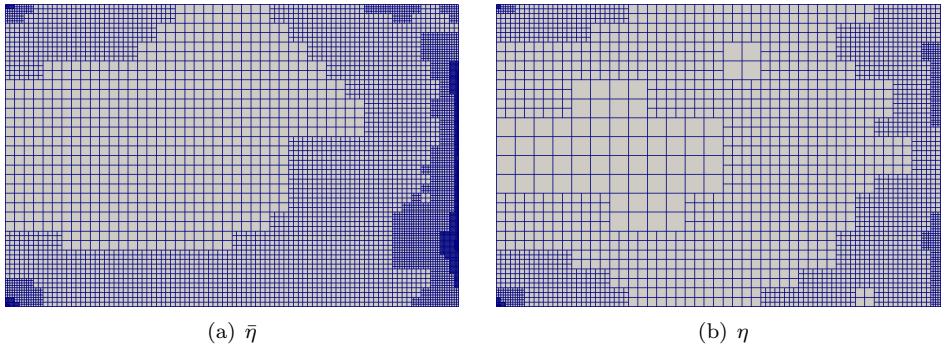


FIG. 8.5. Plot of the relative error w.r.t. the number of mesh cells for the adaptive algorithm based on different error estimators

error estimators $\bar{\eta}_u$, η_u , $\bar{\eta}$, and η , is compared in Figure 8.5. Since the exact value of $J(u)$ is unknown, we approximate this value via extrapolation of functional values on finer uniform meshes. In Figure 8.5, it is obvious that the iteration does not lead to a convergent scheme. Thus, the error estimator $\bar{\eta}_u$ is not suitable to be used as refinement indicator. The very small relative error in the third iteration of $\bar{\eta}_u$ results from a coincidental encounter of the approximated value and the reference value. The results for η_u looks nice in the beginning, but due to the missing refinements in the interior of the domain some accuracy gets lost in the last iterations. For the error estimators $\bar{\eta}$ and η , we obtain similar results. The corresponding value of the quantity of interest converges towards the reference value significantly faster in comparison to the results based on uniform refined meshes. As it is indicated by the adaptive meshes in Figure 8.4, there exist no essential differences between the results of the algorithms based on $\bar{\eta}$ and η .

In the third numerical experiment, the domain is given by $\Omega := [-3, 0] \times [-1, 1]$. We prescribe homogeneous Dirichlet boundary conditions on $\Gamma_D := \{-3\} \times [-1, 1]$

FIG. 8.6. Numerical solution of the third 2D example for $M_\Omega = 24576$ and $M_C = 64$ FIG. 8.7. Adaptive meshes based on different error estimators in the 7th iteration of the adaptive algorithm

and homogeneous Neumann boundary conditions on $\Gamma_N := (-3, 0) \times \{-1, 1\}$. The contact boundary is $\Gamma_C := \{0\} \times [-1, 1]$. Hooke's law with Young's modulus $E := 1$ and Poisson number $\nu := 0.3$ as well as plain strain is applied. The volume force f is set to $f := (0, -0.01)^\top$. The obstacle is given by $\psi := 0.1(x_1 - 1)(x_1 + 1)$. In this experiment, we consider Coulomb friction where s is defined as $s := \mathcal{F}|\sigma_{nn}(u)|$ with the frictional coefficient $\mathcal{F} := 0.4$. The framework as introduced in Section 3 for Tresca friction does not directly fit to Coulomb friction. However, using a simple fix point scheme, we are able to cover Coulomb friction in the following way: For an arbitrary frictional function $s \in L_2(\Gamma_C)$ with $s \geq 0$, we define $(u(s), \lambda_n(s), \lambda_t(s))$ as the unique saddle point of the Signorini problem with Tresca friction, and furthermore, the operator \mathcal{H} as $\mathcal{H}(s) := \mathcal{F}|\lambda_n(s)|$. Assuming that \mathcal{H} has a fix point, i.e., $\mathcal{H}(\bar{s}) = \bar{s}$, we conclude from $\lambda_n = -\sigma_{nn}(u)$ that the saddle point $(u(\bar{s}), \lambda_n(\bar{s}), \lambda_t(\bar{s}))$ fulfills Coulomb friction law. We refer to [8, 10] and references therein for more details on this well-known proceeding.

The numerical solution $(u_h, \lambda_{n,H}, \lambda_{t,H})$ is illustrated in Figure 8.6, where again the von-Mises equivalent stress $\sigma_{M,2}$ with $\sigma_e = 1$ is depicted. We observe high stress values in those areas where boundary conditions change from Dirichlet to Neumann

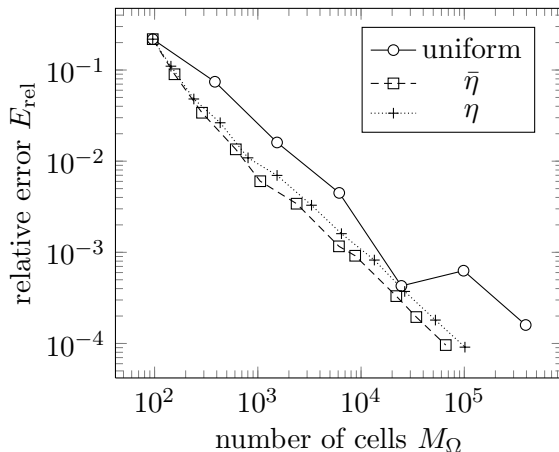


FIG. 8.8. Plot of the relative error w.r.t. the number of mesh cells for the adaptive algorithm based on different error estimators

as well as in the contact zone. As quantity of interest in this example, we choose the energy dissipated by the frictional contact, i.e.

$$J(u, \lambda_t) := -0.1 \int_{\Gamma_C} \lambda_t u_t \, do.$$

In the adaptive algorithm, we use the more flexible optimal mesh strategy described, for instance, in [16] instead of the fixed fraction strategy. The fixed fraction strategy was applied in the foregoing experiments to ensure comparability. The adaptive meshes created in the 7th iteration based on $\bar{\eta}$ and η are presented in Figure 8.7. Both error estimators lead to adaptive refinements in the left corners of the domain and in the contact zone, especially near to the endpoints of the active contact zone. In the interior of the domain, the use of the error estimator $\bar{\eta}$ leads to slightly more adaptive refinements than the use of η . The convergence of the adaptive methods is illustrated in Figure 8.8. The adaptive algorithms lead to better convergence results than the uniform refinement. Only slight differences in the convergence results occur, when $\bar{\eta}$ and η are used.

To demonstrate that our results are also applicable in 3D, we present an example, where the domain Ω is a part of a 3-dimensional disc of radius 1.5,

$$\Omega := \{x \in \mathbb{R}^3 \mid 0.25 \leq x_1^2 + x_2^2 \leq 2.25, |x_3| \leq 0.05, |\arctan(x_2/x_1)| \leq \pi/36\}$$

which is fixed at the inner boundary $\Gamma_D := \{x \in \Omega \mid x_1^2 + x_2^2 = 0.25\}$. The possible contact boundary is given by $\Gamma_C := \{x \in \Omega \mid x_1^2 + x_2^2 = 2.25\}$. Homogeneous Neumann boundary conditions are prescribed on $\Gamma_N = \partial\Omega \setminus (\Gamma_C \cup \Gamma_D)$. Here, we choose the material parameters $E := 10^6$ and $\nu := 0.3$. Volume or surface forces are not applied. The obstacle is parametrized by $\psi := 2x_2^2 - 0.2$. Friction is modelled by the law of Coulomb-Orowan, i.e. $s := \min\{0.15 \cdot \sigma_{nn}, 3 \cdot 10^4\}$, c.f. [20, Section 4.2.5]. The numerical solution is illustrated in Figure 8.9(a), where the von-Mises equivalent stress

$$\sigma_{M,3}(\sigma, \sigma_e) := \frac{\sqrt{\sigma_{11}^2 + \sigma_{22}^2 + \sigma_{33}^2 - \sigma_{11}\sigma_{22} - \sigma_{11}\sigma_{33} - \sigma_{22}\sigma_{33} + 3(\sigma_{21}^2 + \sigma_{31}^2 + \sigma_{32}^2)}}{\sigma_e}$$

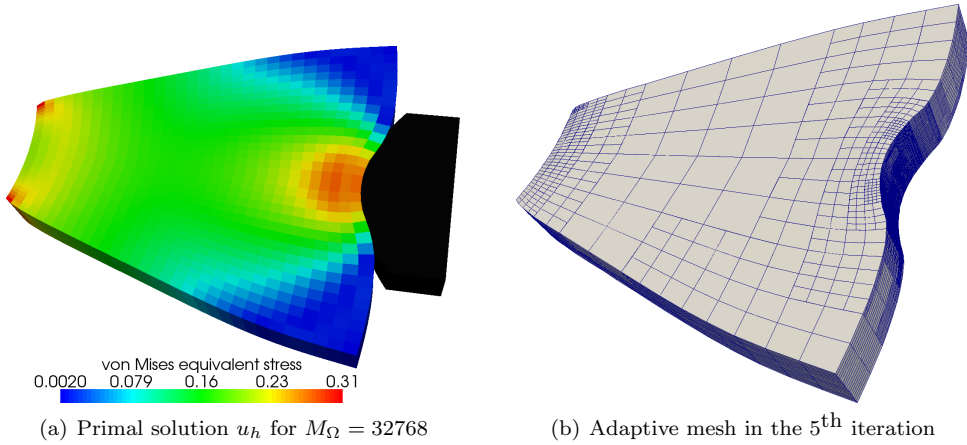


FIG. 8.9. Plot of the 3D primal solution and a corresponding adaptive mesh

with $\sigma_e = 10^6$ is depicted. As the quantity of interest, we apply the functional

$$J(u, \lambda_n, \lambda_t) := 0.1 \sum_{i=1}^3 \int_{B_1} u_i dx + 0.02 \int_{B_2} \lambda_n ds$$

with $B_1 := \{x \in \Omega \mid x_1 \leq 7.5\}$ and $B_2 = \{x \in \Gamma_C \mid |x_2| \leq 1\}$. Note that B_1 is a part of the domain next to the Dirichlet boundary part. The adaptive mesh generated in the 5th iteration of the adaptive algorithm is shown in Figure 8.9(b). We observe local refinements in the contact zone as well as in the region of interest B_1 , which corresponds to our expectations.

9. Conclusions and outlook. In this paper, we present two different goal oriented a posteriori error estimators for static frictional contact problems. Both are based on the DWR method. The first estimator can be used to estimate the error in quantities of interest, which solely depend on the displacement. The second estimator applies to quantities of interest which depend on the displacement *as well as* on the Lagrange multipliers representing the contact forces. In both cases, we obtain the typical terms of the DWR method plus some extra terms resulting from the contact constraints. Both estimators are based on dual problems which imply the quantity of interest. The dual problem defining the first estimator corresponds to the unconstrained contact problem, whereas the dual problem for the second estimator is a mixed problem which is numerically more costly to solve. For both estimators, we apply standard techniques for evaluation and localization. Furthermore, the estimators can be applied within adaptive algorithms.

We study the two estimators in some numerical examples. Both estimators lead to accurate error estimations, if the quantity of interest is defined away from the contact boundary. Due to the poor approximation of the extra terms by the numerical methods, the accuracy is reduced for quantities of interest defined near to the contact boundary. Consequently, the approximation of the extra terms need to be improved. The experiments w.r.t. the adaptive schemes reveal that the error estimator based on the mixed dual problem is much more suited for adaptivity than the estimator based on the non-mixed dual problem, which can lead to non converging schemes. The extension of the second approach to time dependent contact problems is planned

for future work.

Acknowledgement. The authors gratefully acknowledge the financial support by the German Research Foundation (DFG) within the project A5 of the Collaborative Research Centre Transregio 73.

REFERENCES

- [1] W. BANGERTH AND R. RANNACHER, *Adaptive finite element methods for differential equations*, Lectures in Mathematics, ETH Zürich, Birkhäuser, Basel, 2003.
- [2] R. BECKER AND R. RANNACHER, *An optimal control approach to a posteriori error estimation in finite element methods*, Acta Numerica, 10 (2001), pp. 1–102.
- [3] M. BRAACK AND A. ERN, *A posteriori control of modeling errors and discretization errors*, Multiscale Model. Simul., 1 (2003), pp. 221–238.
- [4] D. BRAESS, *Finite Elemente. Theorie, schnelle Löser und Anwendungen in der Elastizitätstheorie*, Springer-Verlag, Berlin, 1997.
- [5] G. DUVAUT AND J. L. LIONS, *Inequalities in mechanics and physics*, Grundlehren der mathematischen Wissenschaften, Springer-Verlag, Berlin, 1976.
- [6] I. EKELAND AND R. TÉMAM, *Convex analysis and variational problems*, Studies in Mathematics and its Applications, North-Holland Publishing Company, Amsterdam, 1976.
- [7] R. GLOWINSKI, *Numerical methods for nonlinear variational problems*, Springer Series in Computational Physics, Springer-Verlag, New York, 1984.
- [8] J. HASLINGER, Z. DOSTAL, AND R. KUCERA, *On a splitting type algorithm for the numerical realization of contact problems with coulomb friction*, Comput. Methods Appl. Mech. Engrg., 191 (2002), pp. 2261–2281.
- [9] J. HASLINGER AND I. HLÁVAČEK, *Approximation of the Signorini problem with friction by a mixed finite element method*, J. Math. Anal. Appl., 86 (1982), pp. 99–122.
- [10] J. HASLINGER AND T. SASSI, *Mixed finite element approximation of 3d contact problems with given friction: error analysis and numerical realization*, Math. Mod. Numer. Anal., 38 (2004), pp. 563–578.
- [11] I. HLÁVAČEK, J. HASLINGER, J. NEČAS, AND J. LOVIŠEK, *Solution of variational inequalities in mechanics*, Applied Mathematical Sciences, Springer-Verlag, New York, 1988.
- [12] N. KIKUCHI AND J.T. ODEN, *Contact problems in elasticity: A study of variational inequalities and finite element methods*, SIAM Studies in Applied Mathematics, SIAM, Society for Industrial and Applied Mathematics, Philadelphia, 1988.
- [13] M. PARASCHIVOIU, J. PERAIRE, AND A. T. PATERA, *A posteriori finite element bounds for linear-functional outputs of elliptic partial differential equations*, Comput. Methods Appl. Mech. Engrg., 150 (1997), pp. 289–312.
- [14] S. PRUDHOMME AND J.T. ODEN, *On goal-oriented error estimation for elliptic problems: Application to the control of pointwise errors*, Comput. Methods Appl. Mech. Engrg., 176 (1999), pp. 313–331.
- [15] A. RADEMACHER, *Adaptive Finite Element Methods for Nonlinear Hyperbolic Problems of Second Order*, PhD thesis, Technische Universität Dortmund, Fakultät für Mathematik (Diss.), Verlag Dr. Hut, München, 2010.
- [16] T. RICHTER, *Parallel Multigrid Method for Adaptive Finite Elements with Application to 3D Flow Problems*, PhD thesis, Ruprecht-Karls-Universität Heidelberg, (Diss.), 2005.
- [17] A. SCHRÖDER, H. BLUM, A. RADEMACHER, AND H. KLEEMANN, *Mixed FEM of higher order for contact Problems with friction*, Int. J. Numer. Anal. Model., 8 (2011), pp. 302–323.
- [18] A. SCHRÖDER AND A. RADEMACHER, *Goal-oriented error control in adaptive mixed FEM for Signorini's Problem*, Comp. Meth. Appl. Mech. Engrg., 200 (2011), pp. 345–355.
- [19] F.T. SUTTMEIER, *Numerical solution of variational inequalities by adaptive finite elements*, Advances in numerical mathematics, Vieweg-Teubner, Wiesbaden, 2008.
- [20] P. WRIGGERS, *Computational Contact Mechanics*, John Wiley & Sons Ltd, Chichester, 2002.